Enhancement of L-Selectin, but Not P-Selectin, Bond Formation Frequency by Convective Flow

Christopher D. Paschall, William H. Guilford, and Michael B. Lawrence
Department of Biomedical Engineering, University of Virginia, Charlottesville, Virginia 22908

ABSTRACT L-selectin-mediated leukocyte rolling has been proposed to require a high rate of bond formation compared to that of P-selectin to compensate for its much higher off-rate. To test this hypothesis, a microbead system was utilized to measure relative L-selectin and P-selectin bond formation rates on their common ligand P-selectin glycoprotein ligand-1 (PSGL-1) under shear flow. Using video microscopy, we tracked selectin-coated microbeads to detect the formation frequency of adhesive tether bonds. From velocity distributions of noninteracting and interacting microbeads, we observed that tether bond formation rates for P-selectin on PSGL-1 decreased with increasing wall shear stress, from 0.14 ± 0.04 bonds/μm at 0.2 dyn/cm^2 to 0.014 ± 0.003 bonds/μm at 1.0 dyn/cm^2. In contrast, L-selectin tether bond formation increased from 0.017 ± 0.005 bonds/μm at 0.2 dyn/cm^2 to 0.031 ± 0.005 bonds/μm at 1.0 dyn/cm^2. L-selectin tether bond formation rates appeared to be enhanced by convective transport, whereas P-selectin rates were inhibited. The transition force for the L-selectin catch-slip transition of 44 pN/bond agreed well with theoretical models (Pereverzev et al. 2005. *Biophys. J.* 89:1446-1454). Despite catch bond behavior, hydrodynamic shear thresholding was not detected with L-selectin beads rolling on PSGL-1. We speculate that shear flow generated compressive forces may enhance L-selectin bond formation relative to that of P-selectin and that L-selectin bonds with PSGL-1 may be tuned for the compressive forces characteristic of leukocyte-leukocyte collisions during secondary capture on the blood vessel wall. This is the first report, to our knowledge, comparing L-selectin and P-selectin bond formation frequencies in shear flow.

INTRODUCTION

Capture and rolling of leukocytes on the blood vessel wall is mediated by the selectin family of adhesion receptors and characterizes the initiation of inflammation (1). During the acute phase of the inflammatory response, leukocyte rolling is governed largely by interactions between P-selectin expressed on the surface of endothelial cells and P-selectin glycoprotein ligand-1 (PSGL-1) on leukocytes (2). In addition, leukocyte L-selectin catalyzes transient aggregation of leukocytes on vascular endothelium through PSGL-1 and other mucin-like ligands expressed by the adherent leukocyte (3–5). The L-selectin-PSGL-1 adhesive interaction frequently results in the incoming leukocyte adhering downstream of a previously adherent leukocyte, a process called secondary capture. In both the primary capture and the secondary capture pathways, the role of the selectin is to initiate adhesion through fast binding reactions.

Experimental measures have shown that in solution P-selectin and L-selectin have rapid on-rates relative to known antibody-antigen reactions (6,7). A three-dimensional (3-D) on-rate of 4.4×10^6 M^{-1}s^{-1} has been determined for P-selectin with PSGL-1 (7). The on-rate constant for L-selectin with soluble glycosylation-dependent cell adhesion molecule-1 (GlyCAM-1), a molecule related to PSGL-1, has been determined to be ~30-fold slower (~10^5 M^{-1}s^{-1}) (6). It should be noted that the selectin ligand was different in each of these experiments (neutrophil-derived PSGL-1 for P-selectin and mouse derived GlyCAM-1 for L-selectin). In contrast, laser trap data suggest that the specific two-dimensional (2-D) on-rates for P-selectin and L-selectin are similar at 1.7 μm^2/s in the absence of physiologic shear forces, although statistical bounds could not be placed on that value (8).

Compounding the differences in estimates of selectin on-rates derived from biochemical and optical trap assays, the analysis of leukocyte rolling on either peripheral node addressing (PNAd) or immobilized GlyCAM-1 has resulted in a diametrically opposed conclusion regarding their relative magnitudes. Since L-selectin off-rates during leukocyte rolling are an order of magnitude higher than those of P-selectin, it has been inferred that L-selectin must have a higher on-rate than P-selectin to maintain stable rolling (9–11). This conclusion was based on a comparison of leukocyte rolling on PNAd or GlyCAM-1 versus P-selectin at equivalent adhesion strengths in a resistance to detachment assay (9). Similarly, the higher neutrophil tethering rate on L-selectin versus P-selectin substrates at comparable site densities has been inferred to represent a higher intrinsic on-rate of L-selectin for PSGL-1 than P-selectin (12).

To estimate the relative tether bond formation rates of P-selectin and L-selectin to their common ligand, PSGL-1, we developed a cell-free assay in which beads coated with selectin could interact discretely with low site density PSGL-1 substrates, thereby allowing visual detection of the formation of selectin tether bonds. The cell-free assay minimizes

Submitted October 5, 2006, and accepted for publication August 27, 2007.

Address reprint requests to William H. Guilford, Dept. of Biomedical Engineering, PO Box 800759, MR5, 1111 415 Lane Road, University of Virginia, Charlottesville, VA 22908. Tel.: 434-924-9908; Fax: 434-982-3870; E-mail: whg2n@virginia.edu.

Editor: Richard E. Waugh.

0006-3495/08/02/1034/12 $2.00

doi: 10.1529/biophysj.106.098707

any effects of cell deformability on selectin binding and increases the likelihood that binding events are governed by small numbers of receptors due to the geometric constraints of the contact patch (13–15). With uniform contact area, it can be inferred that the tether bond formation frequency will scale with the selectin molecular bond formation rate (13,14). To establish objective bounds for the beginning and end of a selectin binding event, we experimentally determined velocity distributions for both noninteracting and interacting particles in the parallel plate flow chamber.

Based on measured velocity distributions, we found that tether bond formation rates for P-selectin decreased over the range of shear stresses 0.2–1.0 dyn/cm^2 (20–100 s^{-1} wall shear rate). In contrast, L-selectin tether bond formation rates, although initially slower than those of P-selectin, increased as flow rates increased. Eventually, L-selectin bead binding rates surpassed those of P-selectin as flow was increased. Despite evidence of catch-slip bond dynamics, L-selectin microbeads failed to give rise to the shear threshold phenomenon as it is manifested with leukocytes and platelets. Our results suggested that convective transport effects enhanced L-selectin bonding frequency with PSGL-1 while inhibiting P-selectin binding to PSGL-1.

MATERIALS AND METHODS

Reagents and protein isolation

Recombinant P-selectin and L-selectin, containing the lectin, epidermal growth factor, and six and two consensus repeat domains, respectively, fused to a human immunoglobulin G (IgG_4), were purchased from R&D Systems (selectin-IgG; Minneapolis, MN). All other reagents were purchased from Sigma (St. Louis, MO).

PSGL-1 was purified from HL-60 cells as previously described (15,16). PSGL-1 purification was verified by sodium dodecylsulfate-polyacrylamide gel electrophoresis and a functional flow chamber assay using the criteria of rolling by HL-60 cells and 300.19 cells transfected with L-selectin. Site densities were estimated by an ELISA-based europium-streptavidin assay (17).

Microbead preparation

Polystyrene microbeads (5.9 ± 0.4 μm) were purchased from Polysciences (Warrington, PA). L-selectin-IgG or P-selectin-IgG was conjugated to the beads using either passive adsorption or carbodiimide chemistry (15). For passive adsorption, beads were washed three times with 0.1 M borate buffer, pH 8.5, and incubated for 4 h with the appropriate selectin-IgG in 0.1 M borate buffer for 4 h at room temperature under end-to-end rotation. After washing with 0.1 M borate buffer, the microbeads were incubated overnight in 1% Tween-20 solution at 4°C under end-to-end rotation to block nonspecific adhesion. For covalent coupling, carboxylate-modified polystyrene microbeads (Polysciences) were prepared following the manufacturer's instructions. The microbeads were incubated in a prescribed amount of L-selectin-IgG or P-selectin-IgG in borate buffer overnight at room temperature with end-to-end rotational mixing (15). The selectin-coated microbeads were then blocked with a Tween-20 solution as described above. Selectin site densities on beads were estimated by flow cytometry using calibrated fluorescent microbeads (18,19).

Before use in the laminar flow chamber assay, the microbeads were centrifuged and resuspended in assay media (Hank's balanced salt solution, 10 mM HEPES, pH 7.4, and 2 mM $CaCl_2$) at a concentration of 5×10^5 beads/ml. As a C-type lectin, $CaCl_2$ is required for selectin binding to PSGL-1 (20).

Flow chamber assay

Polystyrene slides were cut from bacteriological petri dishes (Falcon 1058, Fisher Scientific, Pittsburgh, PA), and diluted PSGL-1 was passively adsorbed to the slide and allowed to incubate at room temperature for 2 h. Slides were blocked for nonspecific adhesion overnight at 4°C with 1% Tween 20 in HBSS. Covalent coupling of PSGL-1 to plastic was found to have no effect on microbead adhesive dynamics (15). The wall shear stress of the parallel plate flow chamber (Glycotech, Rockville, MD) was determined by the gasket dimensions, which were 0.01 inches thick and 1 cm wide. Cell or bead suspensions were drawn into the chamber at room temperature using a PHD 2000 programmable syringe pump (Harvard Apparatus, South Natick, MA) (Fig. 1). The chamber was mounted over an inverted phase-contrast microscope (Diaphot-TMD; Nikon, Garden City, NY) at 40× magnification (1 pixel = 0.185 um).

Counting bead tethers/s was as follows with an adjustment for bond lifetime: $(n-1)/\{(t_n - t_1) - \sum t_{bi}\}$, where n is the number of tether bonds, t_1 is the time of the first tethering event, t_n is the time of the last tethering event in the field of view, and t_{bi} is the duration of the ith tether bond. The recursive formula is valid for $n \geq 2$, as beads with one tethering interaction were excluded from the analysis due to uncertainty as to the time and distance to the next tethering event. Tether bond frequency normalized on a distance basis was estimated by the distance between successive tethers for beads that formed at least two tether bonds in the field of view.

Data acquisition and high speed video analysis

Images from all experiments were recorded using the Photron PCI FastCam (Photron USA, San Diego, CA). The noninterlaced images were stored in the PCI's memory board and transferred directly to the hard drive of a Dell Dimension 8400 (Dell, Austin, TX) in audio video interleave format. High spatiotemporal resolution images (250 frames/s) were loaded into Image J, and particles were tracked using a normalized cross correlation algorithm (21). Centroid interpolation was used to achieve subpixel resolution (22).

Statistical analysis

Data are expressed as the mean ± SE unless otherwise stated. Statistical significance in the differences in bond formation rates for each site density and substrate was verified using a one-way analysis of variance. Values of

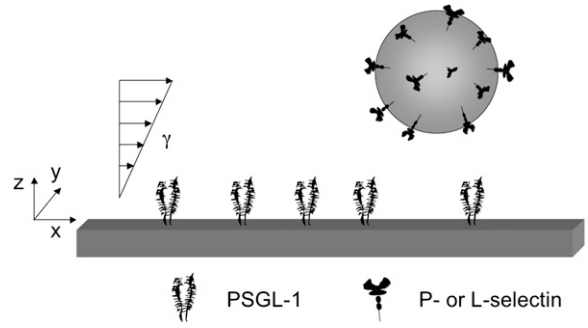

FIGURE 1 Schematic diagram of L-selectin- or P-selectin-coated bead flowing over a PSGL-1 substrate. Recombinant selectin IgG molecules were adsorbed to 6 μm polystyrene microbeads at 500 ng/ml. PSGL-1 was randomly adsorbed to the floor of the flow chamber at bulk concentrations of 1, 10, or 100 ng/ml. Geometrically, microbeads translate convectively in the x-direction, parallel to the floor of the flow chamber. γ = wall shear rate (s^{-1}). Experimentally, the viscosity of the fluid is 1 cP, so that 1 dyn/cm^2 wall shear stress = 100 s^{-1} wall shear rate.

$p < 0.05$ were considered statistically significant. The goodness-of-fit of normal and lognormal distributions of noninteracting beads was assessed using the χ^2 test statistic with $(1 - \alpha) = 0.95$.

RESULTS

Tracking and validation of noninteracting particles

Polystyrene microbeads were coated with identical densities of L-selectin or P-selectin and flowed over a 1% Tween-20-coated plate to determine near-wall, noninteracting particle velocities (Fig. 1). Near-wall velocities followed a linear relationship ($R^2 > 0.99$) with increasing shear stress, agreeing well with the two velocity-flow relationships predicted by the asymptotic analysis and the method of reflections for a bead separation distance of 100 nm (23) (Fig. 2). The good fit of the measured velocities of microbeads with the velocity-flow relationship predicted by the two equations suggested that the beads were within 100 nm of the surface.

Instantaneous velocity fluctuations are frequently used to infer the existence of short-lived selectin bonds between the microbead and surface (10,16,24–26). To assess the impact of spatiotemporal limitations in particle tracking on apparent velocity fluctuations, we calculated the apparent diffusion coefficient of the polystyrene beads in flow. Convective transport dominated bead motion in the direction of flow (the x-direction) (Fig. 1) with a Peclet number > 1000. In the y- and z-directions, negligible convective transport contributed to bead motion and diffusive fluctuations dominated displacements. We collected y-direction displacements and fit them to a Gaussian distribution (Fig. 3 *A*). The distribution had a mean of 0 μm and a standard deviation of 0.025 μm. The root mean-square (RMS) displacement in the y-direction, on small timescales ranging 4–160 ms, provided an estimate of the diffusion coefficient of the microbead. Using the equation $\langle y^2 \rangle = 2Dt$ (27), we obtained a diffusion coefficient of 0.038 ± 0.002 $\mu m^2/s$ by fitting an exponential equation to the experimentally determined diffusion coefficient values at long time points (Fig. 3 *B*). Assuming a bead separation distance of 100 nm from the coverslip, this measurement is higher than the diffusion coefficient of 0.026 $\mu m^2/s$ predicted by simulation using a modified Stokes theory for a bead diffusing near a planar surface (28).

At our highest time resolution, 4 ms (i.e., a single video frame at 125 frames per s), we overestimated the diffusion coefficient (0.081 ± 0.002 $\mu m^2/s$) (Fig. 3 *B*), likely an effect of the low signal/noise ratio (SNR) characteristic of high magnification optical microscopy. At 4 ms time resolution, our measured SNR of 3.5 correlated with detectable error and bias in tracking (21). Expanding the time window for y-displacement observation minimized the effects of shot noise and resulted in a higher SNR (>5). By tracking a nominally stationary bead, we estimated the limit of resolution of our tracking program to be 0.034 μm. Based on this resolution limit and the diffusion coefficient value measured on a time basis of 8 ms, we estimate that our tracking program can theoretically achieve accuracy in velocity measurement to within 0.034 μm/8 ms $\approx$ 4 μm/s. Such velocity uncertainty limits the reliability of bond lifetime measures based solely on small-scale velocity fluctuations, as used in a number of previous studies (25,26,29,30).

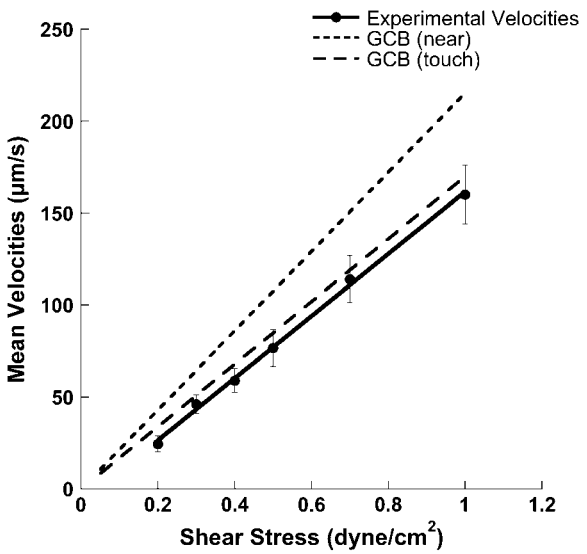

FIGURE 2 Experimentally measured velocities of noninteracting microbeads on a 1% Tween-20-coated surface. Microbeads coated with either P-selectin or L-selectin IgG were flowed over a 1% Tween-20-coated surface to obtain a population of noninteracting velocities. The average velocity is plotted as a function of wall shear stress. Data points represent the average of at least 20 beads in each of three independent experiments (mean ± SE). Average velocities follow a linear relationship with wall shear stress ($R^2 > 0.99$). Theoretical predictions for near-wall velocities using the ''method of reflections'' (*solid line*) and asymptotic, lubrication theory (*dashed line*) outlined by Goldman, Cox, and Brenner (23) are shown.

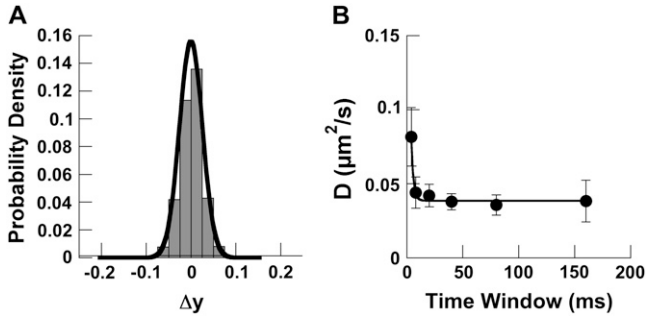

FIGURE 3 Measurement of diffusion of microbeads. (*A*) Distribution of y-displacement (Fig. 1) of noninteracting microbeads in shear flow. The population of displacements is normally distributed with mean 0 μm and standard deviation 0.025 μm ($p < 0.05$). Displacements of exactly zero are included in the 0^+ bin. (*B*) The diffusion coefficient of the microbead was calculated from the RMS displacement in the y-direction using the equation $\langle y^2 \rangle = 2Dt$. Because of interpolation limits in our tracking program, 4 ms time intervals were too small to measure Brownian motion, inflating the diffusion coefficient. By expanding the time window, we were able to compute a diffusion coefficient of 0.038 $\mu m^2/s$. Data shown are the result of at least 15 microbeads (mean ± SE).

Detection of discrete selectin interactions

Beads coated with L-selectin or P-selectin IgG were flowed over a plate coated with either 1 ng/ml, 10 ng/ml, or 100 ng/ml PSGL-1 at a range of shear stresses of 0.2–1.0 dyn/cm^2. Using a europium-streptavidin assay, site densities on the plate varied proportionally with solution concentration and were estimated to be 0.2–20 sites/μm^2 for the range of concentrations tested (17). L-selectin and P-selectin site densities on the bead were determined to be 70 sites/μm^2 using flow cytometry. L-selectin beads interacting with 10 ng/ml PSGL-1 are shown in Fig. 4, *A–F*. Discrete interactions can be visualized as the particle velocity drops below free stream values and is particularly evident at 0.4 dyn/cm^2 wall shear stress and above. Between interactions, beads flow at hydrodynamic velocity matching experimental velocities measured for noninteracting beads, suggesting the absence of adhesive bonds (Fig. 2). No statistically significant differences in interaction frequency or duration were observed between beads coated with L-selectin or P-selectin using either passive adsorption or covalent coupling (data not shown).

To identify a bond formation event, distributions were fit to the experimentally measured velocities of noninteracting particles. A normal distribution fit noninteracting particle velocities at 0.2 and 0.3 dyn/cm^2, whereas a lognormal distribution was fit to beads at 0.4 dyn/cm^2 and above ($p < 0.05$ for each shear stress). Empirically, the distribution of free velocities was well matched by a lognormal distribution, except at the lowest shear stresses, where a normal distribution provided a better match to the data. At the lowest shear stresses, we were unable to collect a significant number of beads far enough from the wall to constitute a lognormal distribution. Most likely, this is due to particle settling before initiation of flow.

A cutoff velocity was established by constructing a 99% confidence interval on the noninteracting velocity distributions for each shear rate to rigorously separate bonding interactions from Brownian motion in the z-direction or other sources of random particle movement. The lower bound of the interval ($\alpha = 0.005$) was used as the critical velocity, which necessarily is a function of the local flow profile, particle size, and distance from the surface. At or below this critical velocity, there was a more than 99% chance that the bead was outside the bounds of normal velocity fluctuations; and therefore the bead was determined to be in the interacting state. Above the critical velocity, the bead was defined to be noninteracting. It should be noted that a 97% confidence interval had to be constructed at 0.2 dyn/cm^2 ($\alpha = 0.015$ cutoff) since the experimentally measured mean velocity was so close to zero.

The population of interacting beads contained a distinct subpopulation of velocities that fell below the critical velocity derived from the distributions of the noninteracting beads (Fig. 5). An overlay of the curves representing the velocity distributions of noninteracting beads on the population of interacting beads was used to establish the velocity criteria for a bonding event. At the lowest shear stress tested (0.2 dyn/cm^2), interacting velocities were difficult to resolve from the noninteracting distribution. Notably, 1.5% of the noninteracting population of velocities at 0.2 dyn/cm^2 fell below our accuracy limits of 4 μm/s. It is possible for a noninteracting particle undergoing Brownian motion to move near enough to the surface for its velocity to drop sufficiently to be interpreted as a bond event, leading to overestimation of the frequency of interactions at the lowest shear stress. At all other shear stresses tested, interacting subpopulations clearly fell outside the best-fit line of the noninteracting distribution (Fig. 5).

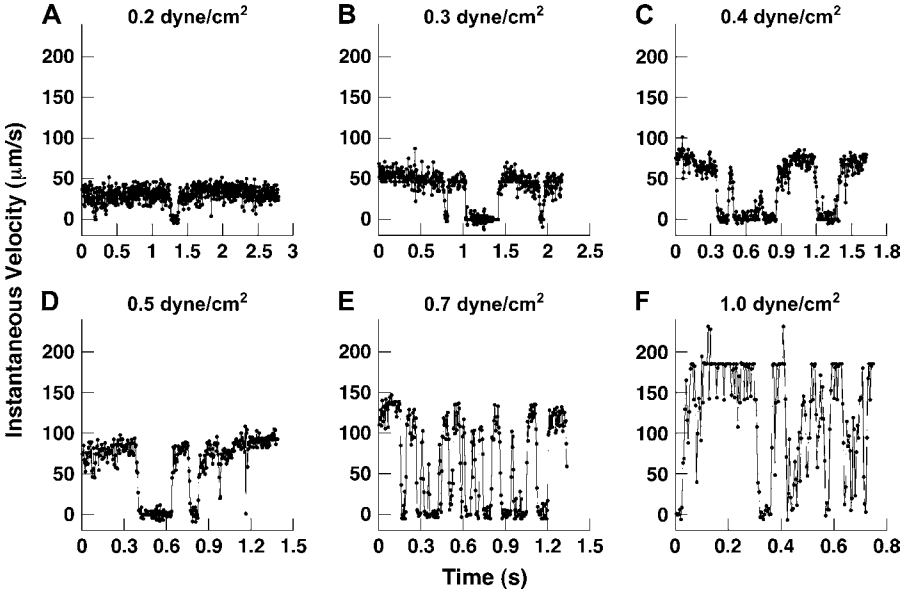

FIGURE 4 Representative individual L-selectin bead histories interacting with PSGL-1 (*A–F*). Microbeads of 6 μm, coated with 500 ng/ml L-selectin IgG, were flowed over a plate coated with 10 ng/ml PSGL-1. Beads drop to velocities near zero when a bond is engaged and return to hydrodynamic velocity between bond events. Velocities were recorded at 250 fps with a 40× objective (1 pixel = 0.185 μm). Similar measurements were taken with L-selectin at 1 and 100 ng/ml and P-selectin (not shown).

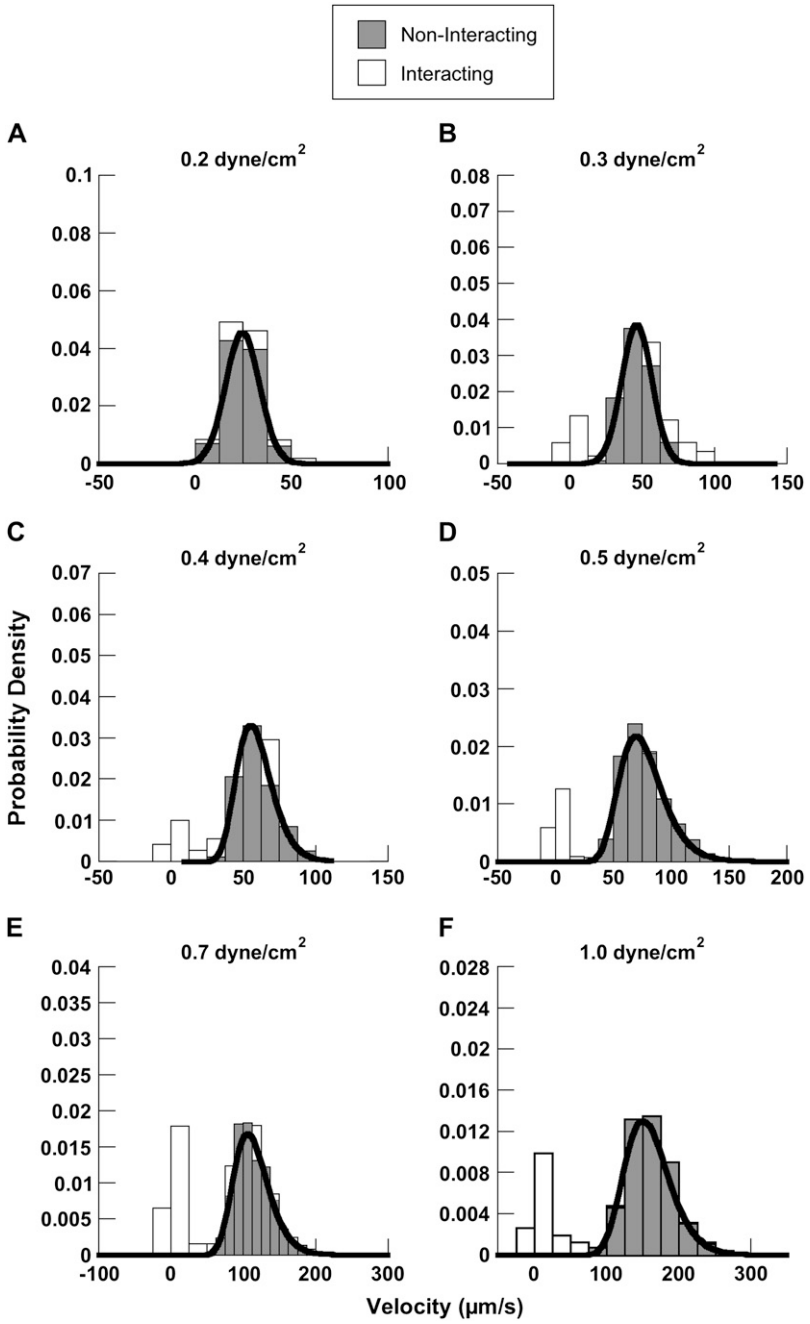

FIGURE 5 Velocity distributions of interacting and noninteracting microbeads. Velocities of 6 μm noninteracting microbeads are plotted in a histogram (*shaded*). A normal (*A* and *B*) or lognormal (*C–F*) distribution was fit to each population. Goodness of fit was assessed using a χ^2 test with $p < 0.05$ for each wall shear stress. As an example, velocity populations from 6 μm beads coated with 500 ng/ml L-selectin interacting with 10 ng/ml PSGL-1 are shown (*open*). A bimodal distribution is obtained with the interacting beads. One part of the population closely resembles the noninteracting beads, and the other population lies to the left of the best-fit line (*black*). This subpopulation of interacting velocities falls outside of the 99% confidence interval and, thus, is a population of bond events.

Comparison of L-selectin and P-selectin tether bond formation rates and tether bond lifetimes

With the establishment of a statistically determined bond event, we set out to compare the bead binding rates (tether bond formation rates) of P-selectin and L-selectin with their common ligand, PSGL-1. A bead binding rate based on an event per time basis (Fig. 6, *A* and *B*) was used to characterized the flux of beads, as it was sensitive to both the bond lifetime as well as the probability that the bead would form subsequent interactions after the initial tether bond. The binding rate on a per time basis was determined by counting the number of interactions in a time window spanning the initiation of the first binding event to the end of the last binding event within the field of view minus the duration of the bonds. This method may overestimate the true bond formation rate on the per time basis, especially for those beads with infrequent interactions. The large majority of beads generated more than two interactions in the field of view (>90% for all cases), and the overestimation diminishes as more interactions are observed.

Binding events normalized on an event per distance basis (Fig. 6, *C* and *D*) report the distance between repeated interactions of the microbead as it flows over the PSGL-1 surface. Bead binding normalized on a per distance scale most closely approximates a chemical kinetic rate. In both measurement approaches, beads (less than 10% of the near-wall population) that had only one interaction in the microscope field of view were discarded from the analysis pool because of the uncertainty of the distance or time before the next successful tethering event. The effect of discarding the single interaction population may result in a slight overestimation of the tether bond frequencies.

For L-selectin, tether bond formation rates increased on both the per time (s^{-1}) and per distance (μm^{-1}) scale with shear stress (Fig. 6, *A* and *C*). At the lowest site density of PSGL-1 (1 ng/ml adsorption concentration, ~0.2 sites/μm^2), L-selectin tether bond formation rates increased from 0.83 ± 0.2 s^{-1} up to 1.8 ± 0.2 s^{-1} and from 0.018 ± 0.005 μm^{-1} up to 0.031 ± 0.005 μm^{-1}. At a higher site density of 100 ng/ml PSGL-1 (~20 sites/μm^2), L-selectin bond formation rates increased from 4.1 ± 2 s^{-1} up to 17.2 ± 3 s^{-1} and from 0.13 ± 0.05 μm^{-1} to 0.18 ± 0.04 μm^{-1} (Fig. 6, *A* and *C*). As flow was increased, L-selectin beads were observed to reattach with increasing frequency on the two highest densities of PSGL-1. At the lowest density of PSGL-1, the frequency of L-selectin bead bond formation was relatively insensitive to increasing flow.

For P-selectin, bond formation rates decreased monotonically over the range of shear stresses and site densities tested on both the per time and per distance scale (Fig. 6, *B* and *D*).

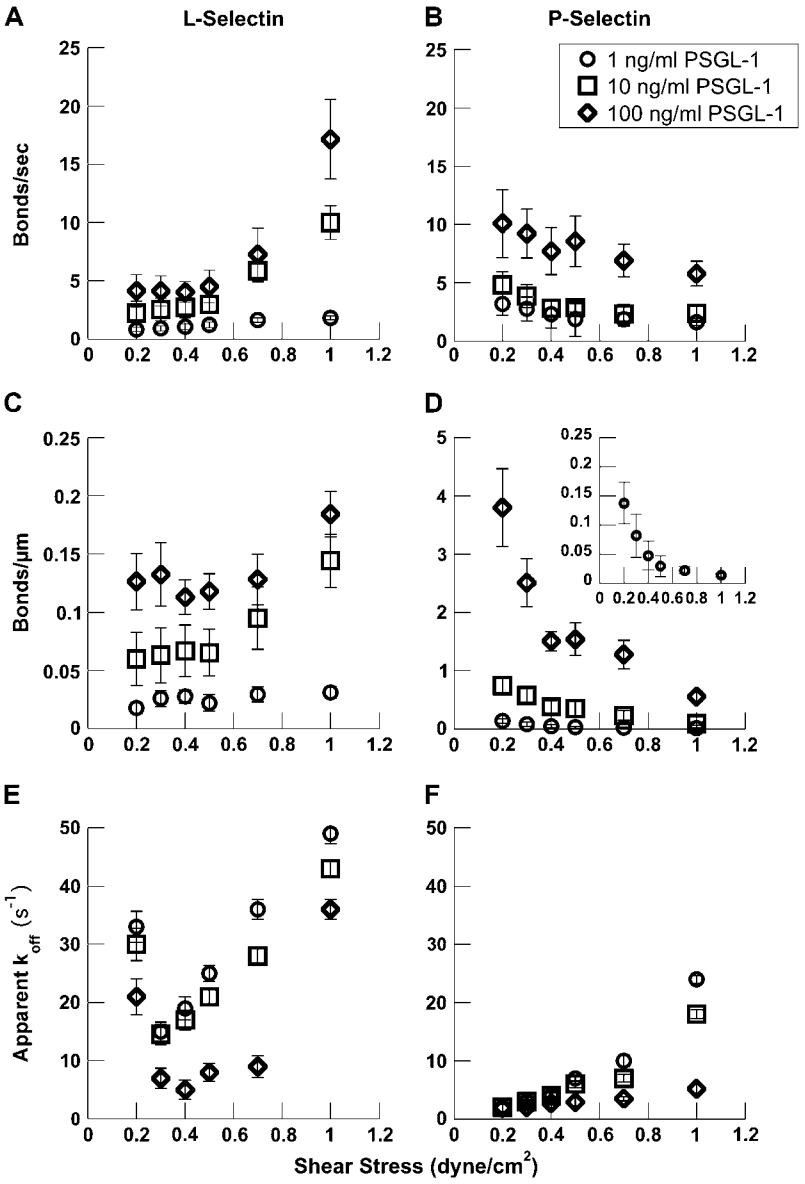

FIGURE 6 Bond formation rates and apparent off-rate of L-selectin or P-selectin microbeads interacting with PSGL-1. L-selectin- (*A* and *C*) or P-selectin- (*B* and *D*) coated microbeads were flowed over 1 ng/ml (*circles*), 10 ng/ml (*squares*), or 100 ng/ml (*diamonds*) PSGL-1 over a range of wall shear stresses. Using statistically determined definitions, bond formation rates were measured on a per time (*A* and *B*) or per distance (*C* and *D*) scale. Note that the *y* axes are different for *C* and *D*. The bond formation rates increased for L-selectin and decreased for P-selectin over the range of wall shear stresses tested. The inset in *D* shows bond formation rates for P-selectin on 1 ng/ml PSGL-1 using the same scale as *C*. At 1 and 10 ng/ml, P-selectin had the higher bond formation rate up to 0.7 dyn/cm^2 wall shear stress. Above 0.7 dyn/cm^2, L-selectin had the higher rate. Apparent off-rates were measured (*E* and *F*) and, at each PSGL-1 site density, the apparent off-rate for L-selectin was 2–10-fold higher than P-selectin. Catch bond behavior was recorded for L-selectin at all PSGL-1 site densities, but not for P-selectin.

P-selectin bond formation rates were significantly higher than for L-selectin below 0.7 dyn/cm^2 wall shear stress. At 1 ng/ml PSGL-1, P-selectin bond formation rates dropped from 3.2 ± 1 bonds/s (0.14 ± 0.04 bonds/μm) at 0.2 dyn/cm^2 to 1.6 ± 0.3 bonds/s (0.014 ± 0.003 bonds/μm) at 1.0 dyn/cm^2. At 100 ng/ml, bond formation rates dropped from 10.1 ± 1 (s^{-1}) (3.8 ± 1 μm^{-1}) at 0.2 dyn/cm^2 to 5.8 ± 1 s^{-1} (0.55 ± 0.1 μm^{-1}) at 1.0 dyn/cm^2. For discrete P-selectin interactions with PSGL-1, these data represent a 1.7–1.9-fold decrease of the bond formation rates on a per timescale and a 6.9–10-fold decrease on the per distance scale. Normalization by the time basis showed a smaller decrease with increasing flow because of the compensatory effect of a greater flux of beads of P-selectin beads compared to L-selectin beads. Individual P-selectin beads were always less likely to form attachments as flow was increased and the distance between binding events increased precipitously for even the highest PSGL-1 density at wall shear stresses of 0.7 dyn/cm^2 and above (Fig. 6 *D*), in contrast to the case with L-selectin.

L-selectin at the highest PSGL-1 density tested supported a significantly higher probability of bead recapture subsequent to forming a tether bond than did P-selectin at 1.0 dyne/cm^2 wall shear stress. P-selectin beads were less likely to immediately reattach to PSGL-1 as flow was increased (Fig. 6 *A* compared to *B*).

Comparison of L-selectin and P-selectin tether bond lifetimes

Using the statistical definition of a bond formation event (Fig. 5), we compared the tether bond lifetimes of P-selectin and L-selectin microbeads to previous work as a control for the internal consistency of our bond lifetime measures (24,25,31). Off-rate constants were determined from the cumulative pause time distribution using 4-ms bins. Receptor-ligand dissociation kinetics follows the relationship $-dC/dt = k_{off} C$, where C is the concentration of receptor-ligand complexes (see Supplementary Material). The natural logarithm of the number of events remaining bound was plotted as a function of time, and the slope of the line was determined to be the off-rate (32). Excluding the shortest pauses or increasing bin size did not alter apparent off-rate values. It was important to establish that our criteria for a definition of a bonding event met several previously established tests, most significantly that of quantal behavior suggestive of either single bonds or uniform-sized bond clusters and that of the recombinant selectin receptors functioned consistently with the native forms reported in previous studies (16,26,33–36).

The apparent off-rates of L-selectin beads on PSGL-1 were calculated from the duration of discrete interactions (Fig. 6 *E*). There were no statistically significant differences ($p > 0.2$) in the off-rate measured at 1 ng/ml (~0.2 sites/μm^2) or 10 ng/ml PSGL-1 (~2.0 sites/μm^2), indicating few multivalent interactions. At all shear stresses, the apparent off-rate at 100 ng/ml PSGL-1 (~20 sites/μm^2) was lower than the other site densities ($p < 0.05$), suggesting the presence of some multivalent interactions (37,38). We observed catch-slip bond behavior for L-selectin-PSGL-1 interactions at all site densities as shown by the drop in apparent off-rate from 0.2 dyn/cm^2 to 0.3 dyn/cm^2 followed by an exponential increase with increasing wall shear stress (Fig. 6 *E*). The minimum of the off-rate curve was located at a shear stress of 0.3 dyn/cm^2 for the two lower site densities and at 0.4 dyn/cm^2 at the highest site density. Using previously described methodologies (15) and assuming a tether arm length of 100 nm based on the combined selectin-PSGL-1 bond length, a wall shear stress of 0.3 dyn/cm^2 corresponds to a 33 pN force on the bond and 0.4 dyn/cm^2 wall shear stress corresponds to a 44 pN force on the bond.

No statistically significant differences were measured in the apparent off-rate of P-selectin on PSGL-1 at wall shear stresses below 0.5 dyn/cm^2 for all site densities tested ($p > 0.05$), suggesting that we were measuring single bonds—or at least small numbers of bonds that in aggregate behave with population dynamics of single bonds (Fig. 6 *F*). The values of the P-selectin off-rate at the lowest PSGL-1 density compare well with previous observations (15). Statistically significant differences were measured for the apparent P-selectin off-rate above 0.5 dyn/cm^2 for the two highest PSGL-1 site densities (100 and 10 ng/ml) ($p < 0.05$). At the highest PSGL-1 site density (100 ng/ml; ~20 sites/μm^2), the apparent off-rate measurements indicate that we are likely observing a mixture of mono- and multivalent interactions. Optical noise limited our ability to resolve discrete bond interactions at shear stresses below 0.2 dyn/cm^2, the regime in which catch bonds have been observed for P-selectin (31).

L-selectin and P-selectin bead flux

To assess the macroscopic behavior of L-selectin and P-selectin beads rolling on PSGL-1, we measured bead rolling flux (the number of rolling beads/area in 1 min) on 250 ng/ml PSGL-1 (Fig. 7). The bead flux measure reports a combination of bead tethering frequency and duration of interaction. We used two methods to introduce beads into the flow chamber. One previously described procedure is referred to here as the ramp method; it required the beads to undergo a presettling interaction at <0.2 dyn/cm^2 wall shear stress before adhesion was measured after step increases in wall shear stress (30,39). The second procedure we used is described as the washout method. With this method, the flow chamber was completely cleared of beads between increases in shear stress, and the beads were allowed to flow into the chamber for 3 min before counting. This method reproduced the protocol for analyses of leukocyte-tethering frequency and accumulation rates performed in many laboratories (40,41).

A monotonic decrease in rolling bead flux as assayed by the washout method was observed for both L-selectin and P-selectin beads as flow was increased from 0.2 to 1.0 dyn/cm^2

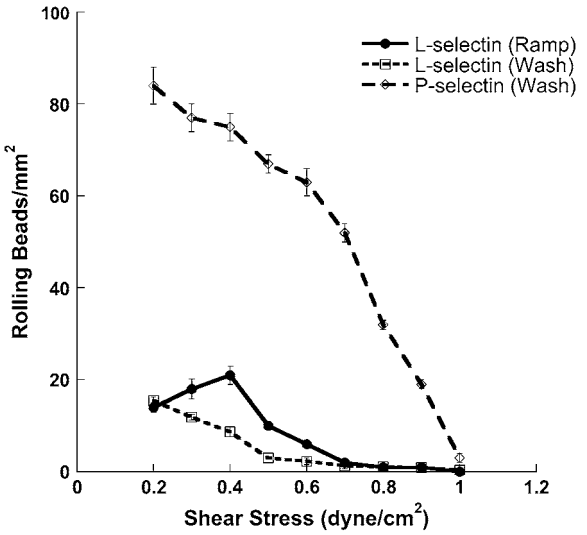

FIGURE 7 L-selectin and P-selectin bead flux measurement on PSGL-1. Microbeads (500 ng/ml L-selectin or P-selectin coated) were flowed over a 250 ng/ml PSGL-1-coated surface. The number of beads rolling in 10 fields-of-view within 1 min was counted using two different methods. A bead was considered rolling if at least five bond events took place in five cell diameters of movement. In the wash method (*dashed*), beads were completely clear from the floor chamber before increasing the wall shear stress. In the ramp method (*solid*), beads were not cleared from the flow chamber in between shear stress increases.

wall shear stress (Fig. 7). The P-selectin microbead rolling flux was significantly higher than that of L-selectin beads for wall shear stresses up to and including 1.0 dyn/cm^2. The P-selectin bead rolling flux was most dramatically greater than that of L-selectin in the ranges where P-selectin microbead binding frequency was greater than that of L-selectin (compare Fig. 6, *C* and *D*, high site density curves). As L-selectin tethering frequency increased relative to P-selectin with increasing flow, the gap between L-selectin and P-selectin bead rolling fluxes closed.

The greater lifetime of P-selectin-PSGL-1 tether bonds at low shear stresses (< 0.6 dyn/cm^2) amplified the effect of the higher probability of P-selectin tether bond formation relative to L-selectin, resulting in a much higher P-selectin bead flux (the number of beads rolling/area). As the P-selectin bond/μm formation rate dropped with increasing flow and the L-selectin bond/μm formation rate increased, the gap between P-selectin and L-selectin bead fluxes narrowed to the point where the bead fluxes were almost identical at 1.0 dyn/cm^2 wall shear stress.

With the ramp method we observed that the L-selectin bead flux increased as flow was stepped to 0.3 and then to 0.4 dyn/cm^2 wall shear stress. Above 0.4 dyn/cm^2, the L-selectin bead flux decreased with increasing flow. The increase in the number of L-selectin beads rolling between 0.2 dyn/cm^2 and 0.4 dyn/cm^2 followed the pattern expected for L-selectin-mediated shear thresholding of leukocytes, though the changes between 0.2 and 0.3 dyn/cm^2, and 0.3 dyn/cm^2 and 0.4 dyn/cm^2 did not meet significance as assessed through a paired Student's *t*-test ($p > 0.1$) (Fig. 7). The rapid attenuation of L-selectin bond lifetimes with increasing shear and the depletion of near-wall microbeads appeared to have muted the impact of flow-enhanced tethering frequency. For L-selectin, the maximum bead rolling flux occurred between wall shear stresses of 0.2 and 0.4 dyn/cm^2. In a cell system, the maximum rolling flux is typically observed in the wall shear stress range of 0.7–1.0 dyn/cm^2 (42,43).

DISCUSSION

The focus of this study was to determine the relative tether bond formation rates of P- and L-selectin under conditions that might give insight into the role PSGL-1 plays in both secondary capture of leukocytes on the blood vessel wall and in mediating capture events directly to P-selectin-expressing endothelium. Unique to our approach was directly comparing L-selectin and P-selectin tether bond formation rates with their common ligand, PSGL-1, in a system in which all the receptors were immobilized and therefore constrained to interact in two dimensions (33,44). By immobilization on a microbead, L- or P-selectin could interact with substrate-anchored PSGL-1 under identical hydrodynamic conditions.

Impact of convective transport on selectin tether bond formation rates

Unexpectedly, L-selectin and P-selectin bond formation rates were strongly but oppositely influenced by convective transport. Apparent bond formation rates for P-selectin, as assessed from the frequency of bead interactions with the PSGL-1-coated substrate, declined steadily as flow increased until successful bead binding events became undetectable at wall shear stresses above 1.0 dyn/cm^2. In contrast, L-selectin formation rates were much lower than those of P-selectin below 0.7 dyn/cm^2 (70 s^{-1}) wall shear stress. Above 0.7 dyn/cm^2, convective effects became dominant and L-selectin rates surpassed those of P-selectin.

The prevailing paradigm in the immunological literature suggests that the on-rate for L-selectin must be higher than P-selectin to maintain stable rolling since the unstressed off-rate for L-selectin is 7–10-fold higher than P-selectin (9,11, 36,45). Given the similarity of hydrodynamic and transport effects between the leukocyte rolling assay and our microbead rolling assay, we expected bond formation probabilities for L-selectin to be higher than those for P-selectin. However, we found that to be true only at a wall shear stress of 0.7 dyn/cm^2 and above. Biochemical assays, in contrast, suggest that in the absence of hydrodynamic forces, the P-selectin-PSGL-1 on-rate is more than an order of magnitude higher than L-selectin with the high endothelial venule ligand, GlyCAM-1 (6,7). In our assay system incorporating hydrodynamic forces, the enhancement of L-selectin on-rates by

shear coupled with the inhibition of P-selectin on-rates appeared to reconcile these two disparate observations.

Adhesion receptor binding probability has been proposed to be a function of the applied force on the bond, with some modeling approaches suggesting force inhibits binding and others suggesting force may enhance binding (13,14,46–50). Recently, it was shown that neutrophil binding probability to ICAM-1 increased linearly with contact stress, underscoring the importance of force in adhesive bond formation processes (47). In the bead assay, as flow is increased the potential compressive force on any newly formed bond will increase substantially along with increases in proximate receptors and ligands. To explain the significant increases in L-selectin bond formation with flow, we hypothesize that the on-rate for the L-selectin-PSGL-1 bond is a function of applied compressive force and that, contrastingly, the on-rate for the P-selectin-PSGL-1 bond is a very weak function of compressive force or is essentially constant. In support of this concept, it has recently been shown that L-selectin bonds have a higher mechanical spring constant than P-selectin bonds (46). Mathematical models predict that bonds with higher spring constants respond more rapidly to applied external forces (14). Also consistent with our hypothesis, it has been speculated that the on-rate for P-selectin-PSGL-1 bonds may be insensitive to compressive load and, thus, more highly dependent on the encounter time between ligand and receptor than the on-rate for L-selectin-PSGL-1 bonds (51).

Relative effects of convection and diffusion on selectin tether bond formation

The Peclet number for a surface-anchored adhesion molecule predicts whether convective transport plays a prominent role in binding relative to diffusive transport (13,28). If we take U to be the translational velocity of the sphere in shear flow, R to be the sphere radius, and Ω to be the rotational velocity, we can compute a slip velocity, v, where $v = U - R\Omega$ (21). In our case, $v \sim 0.5U$, so that, for a 6-μm sphere, we obtain a slip velocity of ~13–75 μm/s over our range of tested shear stresses. Based on the diffusivity of a protein anchored to a cytoskeleton (10^{-11} cm^2/s) and a characteristic length of the receptor (~100 nm) and using the equation Peclet = [characteristic length][slip velocity]/[receptor diffusivity], we calculate a Peclet number of ~1300–7500 for the receptor on the surface of the bead, suggesting the importance of convective transport. Nevertheless, diffusion processes may still be important for the adhesion receptor's binding pockets to find each other and ''close the deal''. It should be recognized that when adhesion molecules are immobilized their length and multidomain structure may still allow considerable mobility of the binding pocket. The difference between an immobilized and free receptor is that the diffusive transport of the binding pocket becomes dependent on the length and mobility of the receptor's domains rather than the diffusivity of the entire molecule. Obviously, beads do not precisely simulate the diffusive behavior of receptors in the phospholipid bilayer of the cell membrane. However, PSGL-1 has a high degree of cytoskeletal association (52,53) and may not freely diffuse enough to be able to measure substantially different molecular kinetics.

Consistent with the analysis of Chang and Hammer (13), our data strongly support a model in which the relative motion of two surfaces enhances receptor binding probability, at least for L-selectin. P-selectin-PSGL-1 bonds may, in contrast, be much more highly sensitive to encounter time and therefore less likely to be amplified by convective transport. Given the smaller spring constant for P-selectin (46), we would expect a slow force response to manifest itself in a bond formation probability more dependent on encounter time.

Dependence of leukocyte hydrodynamic shear thresholding on selectin catch-slip bonds

It has been suggested that catch-bonds are responsible for the L-selectin shear threshold phenomenon (25,31). The phenomenon is typically characterized by an increase in cell rolling flux that peaks in the range of 0.7–1.0 dyn/cm^2 wall shear stress. Interestingly, the peak of the leukocyte shear threshold curve does not match the minimum in the off-rate data for either L-selectin (Fig. 6 *E*) or P-selectin (31). Theoretical models have predicted that the L-selectin catch-slip transition (the minimum in the off-rate) should occur at a bond force of ~48 pN (54), which agrees well with our experimental measurements of 45 pN for the catch-slip transition of L-selectin-PSGL-1. Other investigators have reported that the catch-slip transition takes place at 110 pN (25). The discrepancy between our measures and previous work may be due to the low frequency of multivalent interactions between L-selectin with PSGL-1 in our assay design. Supporting the possibility of high levels of multivalency in previous studies is the inability of microbeads to reach hydrodynamic velocity between tether bond formation events (25).

Assuming that single bonds govern cell adhesion and that catch bonds play a significant role in the manifestation of the shear threshold phenomenon, it would be expected that the peak of the shear threshold curve would match the minimum in the off-rate data. Since we were unable to observe bead shear thresholding experimentally in an interaction dominated by single bonds, it is possible that multiple contacts are formed in a cell system, possibly as a result of cell deformability or the presence of microvilli. If multiple bonds are present during a leukocyte tethering event, the load would be distributed and it is possible that each bond, individually, would fall into the catch-bond regime. We cannot, at this time, directly match the findings from our cell-free assay to a cell system because of uncertainties in the bond numbers in the contact zone of each system. Nevertheless, our data

suggest that although catch bonds may be important, other factors such as force-amplified bond formation by way of convective transport (13,26,43) or shear dependent increases in bond number (55) may make significant contributions to shear thresholding.

Impact of Brownian motion on the estimation of bond lifetime and tether bond formation frequency

As part of this study, we developed a statistical framework for analyzing velocity fluctuations to assess the frequency and duration of selectin bonding events. Other groups have used acceleration fluctuations to determine lifetimes of events (25) or velocity thresholds based on an arbitrary percentage (usually 50%) of theoretical hydrodynamic velocity (30). In both of these approaches, the deviation from the normal velocity fluctuations of a noninteracting particle is used to determine the beginning and end of a bonding event. However, due to limitations in tracking at high video acquisition rates, we were unable to resolve discrete bond events using an acceleration threshold, especially at low shear stresses. The 50% velocity threshold approach also proved problematic at high video acquisition rates due to a combination of optical noise and Brownian motion of the flowing beads. Brief bonding events may appear indistinguishable from the velocity fluctuations as particles diffuse into faster or slower streamlines near the wall.

We addressed the problem of real and apparent Brownian motion effects on bead velocity fluctuations by generating velocity distributions in flow of both bare and selectin-coated microbeads. The distributions captured the variation in microbead velocity that occurred due to both apparent and real Brownian motion as well as adhesion bond formation. Using the corrected bead diffusion coefficient and measured tracking noise of ± 34 nm allowed us to conclude that our particle tracking was accurate to 4 μm/s. Velocities ≤ 4 μm/s therefore could not be reliably interpreted as a bond formation event. Causes of the discrepancy between our experimental diffusion coefficients and the theoretical modified Stokes-Einstein approximation may include environmental factors such as surface roughness and unsteadiness of flow.

Relationship between bead rolling flux and apparent tether bond formation rates

It may seem paradoxical that we observed an increase bond formation rate for L-selectin on PSGL-1 and, at the same time, a decrease in rolling flux over the range of shear stresses tested. It should be noted that the initial contact of a leukocyte or selectin-coated microbead and subsequent rolling contact appear to be distinct events, with the former requiring capture from free flow and the latter resulting advantageously from the lower separation distances and slip velocities between the surface-bound ligands (56–58). The flux measurements provided us with an indicator of how well L- or P-selectin established the first adhesion of the microbead to the PSGL-1 substrate. From our data, increasing shear decreases the probability that the first successful contact will be made in both L-selectin and P-selectin binding. However, once the first contact is made, shear enhances bond formation rates between the bead and substrate with L-selectin but not P-selectin. Taken together, our data highlight the importance of individual bead histories in measuring bond formation rates.

The extrapolation of bead adhesive dynamics to a specific on-rate constant will require both model and experiment to more fully characterize the time-variant interaction zone during bead tethering and rolling in flow. Although it is not currently possible to extract a specific 2-D on-rate from the bead assay as described in this report, we were able to observe the effects of convective transport on P- and L-selectin tether bonding frequencies in a system in which the contact area, encounter time, and respective surface ligand densities were identical. To estimate the specific 2-D kinetics of adhesion receptor binding, we would need at a minimum the accurate determination of the area of interaction, the time of interaction, and the number of molecules available for interaction. Previous work using micropipette binding frequency analysis has generated binding probability curves that can relate binding frequency of surface-immobilized IgG with cell surface CD16A to an estimate of the on-rate, given assumptions of contact area, site densities, and the known solution phase affinity of the interaction (59,60). A similar approach using PSGL-1-expressing cells and immobilized P-selectin has further suggested that 3-D kinetics and 2-D kinetics are sensitive to molecular orientation in some assay systems (33). Given the challenges of converting the solution phase affinity for selectins to two dimensions, the large uncertainties of accurately determining the contact area-time relationship, plus the possibility that the 2-D affinity of a selectin might be different under flow conditions, we chose to focus on the dynamic adhesion behavior of cell-sized microbeads to report selectin tether bond formation rates.

CONCLUSIONS

Our data present several interesting possibilities for future studies. We have shown that, for L-selectin-PSGL-1 interactions, convective transport enhances bond formation rates after the first bond has been formed. Physiologically, L-selectin-PSGL-1 interactions in postcapillary venules mediate leukocyte secondary capture, an amplification mechanism for adhesion to endothelium (5,61,62). It is uncertain at this point whether these unique properties of the L-selectin-PSGL-1 bond facilitate adhesion at high shear stresses or if shear-induced increases in bond number play a role in successful secondary capture events. Because of the deformability of a cell, increases in shear stress could increase the number of available bonds with the reaction area, thereby boosting the probability that the first bond could form.

In summary, this work highlights two key components of the nature of P-selectin and L-selectin interactions with PSGL-1. First, the on-rate for L-selectin interactions appeared more sensitive to compressive load compared to that of P-selectin. Second, the on-rate for P-selectin was significantly higher than that of L-selectin at low shear stresses but not at higher flow rates where secondary capture mechanisms dominate leukocyte tethering (63). The amplification of L-selectin-PSGL-1 binding rates by shear and induced compressive forces may in part determine whether leukocyte primary capture (governed by P-selectin-PSGL-1 interactions) or secondary tethering (controlled by L-selectin-PSGL) is the principal mechanism by which leukocytes are recruited to the vessel wall.

SUPPLEMENTARY MATERIAL

To view all of the supplemental files associated with this article, visit www.biophysj.org.

We thank Brian Schmidt for helpful discussions on small-scale particle motions. A preliminary version of this manuscript was presented at the Annual Biomedical Engineering Society Meeting, Oct. 4, 2005.

This work was supported by the National Institutes of Health (HL054614).

REFERENCES

1. Lawrence, M. B. 1999. Selectin-carbohydrate interactions in shear flow. *Curr. Opin. Chem. Biol.* 3:659–664.
2. Ley, K., editor. 2001. Physiology of Inflammation. Oxford University Press, New York.
3. Walcheck, B., K. L. Moore, R. P. McEver, and T. K. Kishimoto. 1996. Neutrophil-neutrophil interactions under hydrodynamic shear stress involve L-selectin and PSGL-1: a mechanism that amplifies initial leukocyte accumulation on P-selectin in vitro. *J. Clin. Invest.* 98:1081–1087.
4. Alon, R., R. C. Fuhlbrigge, E. B. Finger, and T. A. Springer. 1996. Interactions through L-selectin between leukocytes and adherent leukocytes nucleate rolling adhesions on selectins and VCAM-1 in shear flow. *J. Cell Biol.* 135:849–865.
5. Eriksson, E. E., X. Xie, J. Werr, P. Thoren, and L. Lindbom. 2001. Importance of primary capture and L-selectin-dependent secondary capture in leukocyte accumulation in inflammation and atherosclerosis in vivo. *J. Exp. Med.* 194:205–218.
6. Nicholson, M. W., A. N. Barclay, M. S. Singer, S. D. Rosen, and P. A. van der Merwe. 1998. Affinity and kinetic analysis of L-selectin (CD62L) binding to glycosylation-dependent cell-adhesion molecule-1. *J. Biol. Chem.* 273:763–770.
7. Mehta, P., R. D. Cummings, and R. P. McEver. 1998. Affinity and kinetic analysis of P-selectin binding to P-selectin glycoprotein ligand-1. *J. Biol. Chem.* 273:32506–32513.
8. Rinko, L. J., M. B. Lawrence, and W. H. Guilford. 2004. The molecular mechanics of P- and L-selectin lectin domains binding to PSGL-1. *Biophys. J.* 86:544–554.
9. Puri, K. D., E. B. Finger, and T. A. Springer. 1997. The faster kinetics of L-selectin than of E-selectin and P-selectin rolling at comparable binding strength. *J. Immunol.* 158:405–413.
10. Puri, K. D., S. Chen, and T. A. Springer. 1998. Modifying the mechanical property and shear threshold of L-selectin adhesion independently of equilibrium properties. *Nature.* 392:930–933.
11. Rosen, S. D. 2004. Ligands for L-selectin: homing, inflammation, and beyond. *Annu. Rev. Immunol.* 22:129–156.
12. Smith, M. J., E. L. Berg, and M. B. Lawrence. 1999. A direct comparison of selectin-mediated transient, adhesive events using high temporal resolution. *Biophys. J.* 77:3371–3383.
13. Chang, K. C., and D. A. Hammer. 1999. The forward rate of binding of surface-tethered reactants: effect of relative motion between two surfaces. *Biophys. J.* 76:1280–1292.
14. Chang, K. C., D. F. Tees, and D. A. Hammer. 2000. The state diagram for cell adhesion under flow: leukocyte rolling and firm adhesion. *Proc. Natl. Acad. Sci. USA.* 97:11262–11267.
15. Park, E. Y., M. J. Smith, E. S. Stropp, K. R. Snapp, J. A. DiVietro, W. F. Walker, D. W. Schmidtke, S. L. Diamond, and M. B. Lawrence. 2002. Comparison of PSGL-1 microbead and neutrophil rolling: microvillus elongation stabilizes P-selectin bond clusters. *Biophys. J.* 82:1835–1847.
16. Smith, M. J., B. R. Smith, M. B. Lawrence, and K. R. Snapp. 2004. Functional analysis of the combined role of the O-linked branching enzyme core 2 β1–6-N-glucosaminyltransferase and dimerization of P-selectin glycoprotein ligand-1 in rolling on P-selectin. *J. Biol. Chem.* 279:21984–21991.
17. Sang Won Ham, A., D. J. Goetz, A. L. Klibanov, and M. B. Lawrence. 2007. Microparticle adhesive dynamics and rolling mediated by selectin-specific antibodies under flow. *Biotechnol. Bioeng.* 96:596–607.
18. Green, C. E., U. Y. Schaff, M. R. Sarantos, A. F. Lum, D. E. Staunton, and S. I. Simon. 2006. Dynamic shifts in LFA-1 affinity regulate neutrophil rolling, arrest, and transmigration on inflamed endothelium. *Blood.* 107:2101–2111.
19. Lum, A. F., C. E. Green, G. R. Lee, D. E. Staunton, and S. I. Simon. 2002. Dynamic regulation of LFA-1 activation and neutrophil arrest on intercellular adhesion molecule 1 (ICAM-1) in shear flow. *J. Biol. Chem.* 277:20660–20670.
20. Somers, W. S., J. Tang, G. D. Shaw, and R. T. Camphausen. 2000. Insights into the molecular basis of leukocyte tethering and rolling revealed by structures of P- and E-selectin bound to SLe(X) and PSGL-1. *Cell.* 103:467–479.
21. Cheezum, M. K., W. F. Walker, and W. H. Guilford. 2001. Quantitative comparison of algorithms for tracking single fluorescent particles. *Biophys. J.* 81:2378–2388.
22. Gelles, J., B. J. Schnapp, and M. P. Sheetz. 1988. Tracking kinesin-driven movements with nanometre-scale precision. *Nature.* 331:450–453.
23. Goldman, A. J., R. G. Cox, and H. Brenner. 1967. Slow viscous motion of a sphere parallel to a plane wall-I. Motion through a quiescent fluid. *Chem. Eng. Sci.* 22:637–651.
24. Sarangapani, K. K., T. Yago, A. G. Klopocki, M. B. Lawrence, C. B. Fieger, S. D. Rosen, R. P. McEver, and C. Zhu. 2004. Low force decelerates L-selectin dissociation from P-selectin glycoprotein ligand-1 and endoglycan. *J. Biol. Chem.* 279:2291–2298.
25. Yago, T., J. Wu, C. D. Wey, A. G. Klopocki, C. Zhu, and R. P. McEver. 2004. Catch bonds govern adhesion through L-selectin at threshold shear. *J. Cell Biol.* 166:913–923.
26. Schwarz, U. S., and R. Alon. 2004. L-selectin-mediated leukocyte tethering in shear flow is controlled by multiple contacts and cytoskeletal anchorage facilitating fast rebinding events. *Proc. Natl. Acad. Sci. USA.* 101:6940–6945.
27. Benedek, G. B., and F. M. H. Villars. 2000. Physics with Illustrative Examples from Medicine and Biology. Springer, New York.
28. Pierres, A., A.-M. Benoliel, C. Zhu, and P. Bongrand. 2001. Diffusion of microspheres in shear flow near a wall: use to measure binding rates between attached molecules. *Biophys. J.* 81:25–42.
29. Ramachandran, V., M. Williams, T. Yago, D. W. Schmidtke, and R. P. McEver. 2004. Dynamic alterations of membrane tethers stabilize leukocyte rolling on P-selectin. *Proc. Natl. Acad. Sci. USA.* 101: 13519–13524.
30. Greenberg, A. W., D. K. Brunk, and D. A. Hammer. 2000. Cell-free rolling mediated by L-selectin and sialyl Lewis(x) reveals the shear threshold effect. *Biophys. J.* 79:2391–2402.

31. Marshall, B. T., M. Long, J. W. Piper, T. Yago, R. P. McEver, and C. Zhu. 2003. Direct observation of catch bonds involving cell-adhesion molecules. *Nature*. 423:190–193.

32. Alon, R., D. A. Hammer, and T. A. Springer. 1995. Lifetime of the P-selectin-carbohydrate bond and its response to tensile force in hydrodynamic flow. *Nature*. 374:539–542.

33. Huang, J., J. Chen, S. E. Chesla, T. Yago, P. Mehta, R. P. McEver, C. Zhu, and M. Long. 2004. Quantifying the effects of molecular orientation and length on two-dimensional receptor-ligand binding kinetics. *J. Biol. Chem*. 279:44915–44923.

34. Hanley, W. D., D. Wirtz, and K. Konstantopoulos. 2004. Distinct kinetic and mechanical properties govern selectin-leukocyte interactions. *J. Cell Sci*. 117:2503–2511.

35. Zhu, C., M. Long, S. E. Chesla, and P. Bongrand. 2002. Measuring receptor/ligand interaction at the single-bond level: experimental and interpretative issues. *Ann. Biomed. Eng*. 30:305–314.

36. Alon, R., S. Chen, K. D. Puri, E. B. Finger, and T. A. Springer. 1997. The kinetics of L-selectin tethers and the mechanics of selectin-mediated rolling. *J. Cell Biol.* 138:1169–1180.

37. Tees, D. F., R. E. Waugh, and D. A. Hammer. 2001. A microcantilever device to assess the effect of force on the lifetime of selectin-carbohydrate bonds. *Biophys. J*. 80:668–682.

38. Bhatia, S. K., M. R. King, and D. A. Hammer. 2003. The state diagram for cell adhesion mediated by two receptors. *Biophys. J*. 84:2671–2690.

39. Rodgers, S. D., R. T. Camphausen, and D. A. Hammer. 2000. Sialyl Lewis(x)-mediated, PSGL-1-independent rolling adhesion on P-selectin. *Biophys. J*. 79:694–706.

40. DiVietro, J. A., D. C. Brown, L. A. Sklar, R. S. Larson, and M. B. Lawrence. 2007. Immobilized stromal cell-derived factor-1alpha triggers rapid VLA-4 affinity increases to stabilized lymphocyte tethers on VCAM-1 and subsequently initiate firm adhesion. *J. Immunol.* 178:3903–3905.

41. Dwir, O., G. S. Kansas, and R. Alon. 2001. Cytoplasmic anchorage of L-selectin controls leukocyte capture and rolling by increasing the mechanical stability of the selectin tether. *J. Cell Biol.* 155:145–156.

42. Finger, E. B., K. D. Puri, R. Alon, M. B. Lawrence, U. H. von Andrian, and T. A. Springer. 1996. Adhesion through L-selectin requires a threshold hydrodynamic shear. *Nature*. 379:266–269.

43. Lawrence, M. B., G. S. Kansas, E. J. Kunkel, and K. Ley. 1997. Threshold levels of fluid shear promote leukocyte adhesion through selectins (CD62L,P,E). *J. Cell Biol.* 136:717–727.

44. Dustin, M. L., S. K. Bromley, M. M. Davis, and C. Zhu. 2001. Identification of self through two-dimensional chemistry and synapses. *Annu. Rev. Cell Dev. Biol.* 17:133–157.

45. Puri, K. D., and T. A. Springer. 1996. A Schiff base with mildly oxidized carbohydrate ligands stabilizes L-selectin and not P-selectin or E-selectin rolling adhesions in shear flow. *J. Biol. Chem.* 271:5404–5413.

46. Marshall, B. T., K. K. Sarangapani, J. Wu, M. B. Lawrence, R. P. McEver, and C. Zhu. 2006. Measuring molecular elasticity by atomic force microscope cantilever fluctuations. *Biophys. J*. 90:681–692.

47. Spillmann, C. M., E. Lomakina, and R. E. Waugh. 2004. Neutrophil adhesive contact dependence on impingement force. *Biophys. J*. 87: 4237–4245.

48. Li, P., P. Selvaraj, and C. Zhu. 1999. Analysis of competition binding between soluble and membrane-bound ligands for cell surface receptors. *Biophys. J*. 77:3394–3406.

49. Long, M., H. L. Goldsmith, D. F. Tees, and C. Zhu. 1999. Probabilistic modeling of shear-induced formation and breakage of doublets cross-linked by receptor-ligand bonds. *Biophys. J*. 76:1112–1128.

50. Dembo, M., D. C. Torney, K. Saxman, and D. A. Hammer. 1988. The reaction limited kinetics of membrane-to-surface adhesion and detachment. *Proc. R. Soc. Lond. B Biol. Sci.* 234:55–83.

51. Erdmann, T., and U. S. Schwarz. 2004. Stability of adhesion clusters under constant force. *Phys. Rev. Lett*. 92:108102.

52. Snapp, K. R., C. E. Heitzig, and G. S. Kansas. 2002. Attachment of the PSGL-1 cytoplasmic domain to the actin cytoskeleton is essential for leukocyte rolling on P-selectin. *Blood*. 99:4494–4502.

53. Alonso-Lebrero, J. L., J. M. Serrador, C. Dominguez-Jimenez, O. Barreiro, A. Luque, M. A. del Pozo, K. Snapp, G. Kansas, R. Schwartz-Albiez, H. Furthmayr, F. Lozano, and F. Sanchez-Madrid. 2000. Polarization and interaction of adhesion molecules P-selectin glycoprotein ligand 1 and intercellular adhesion molecule 3 with moesin and ezrin in myeloid cells. *Blood.* 95:2413–2419.

54. Pereverzev, Y. V., O. V. Prezhdo, M. Forero, E. V. Sokurenko, and W. E. Thomas. 2005. The two-pathway model for the catch-slip transition in biological adhesion. *Biophys. J*. 89:1446–1454.

55. Chen, S., and T. A. Springer. 1999. An automatic braking system that stabilizes leukocyte rolling by an increase in selectin bond number with shear. *J. Cell Biol.* 144:185–200.

56. Faucheux, L. P., and A. J. Libchaber. 1994. Confined Brownian motion. *Phys. Rev. E Stat. Phys. Plasmas Fluids Relat. Interdiscip. Topics*. 49:5158–5163.

57. Kaplanski, G., C. Farnarier, O. Tissot, A. Pierres, A.-M. Benoliel, M. C. Alessi, S. Kaplanski, and P. Bongrand. 1993. Granulocyte-endothelium initial adhesion. Analysis of transient binding events mediated by E-selectin in a laminar shear flow. *Biophys. J*. 64:1922–1933.

58. Goldman, A. J., R. G. Cox, and H. Brenner. 1967. Slow viscous motion of a sphere parallel to a plane wall-II. Couette flow. *Chem. Eng. Sci*. 22:653–660.

59. Piper, J. W., R. A. Swerlick, and C. Zhu. 1998. Determining force dependence of two-dimensional receptor-ligand binding affinity by centrifugation. *Biophys. J*. 74:492–513.

60. Chesla, S. E., P. Selvaraj, and C. Zhu. 1998. Measuring two-dimensional receptor-ligand binding kinetics by micropipette. *Biophys. J*. 75:1553–1572.

61. Galkina, E., A. Kadl, J. Sanders, D. Varughese, I. J. Sarembock, and K. Ley. 2006. Lymphocyte recruitment into the aortic wall before and during development of atherosclerosis is partially L-selectin dependent. *J. Exp. Med*. 203:1273–1282.

62. Kadash, K. E., M. B. Lawrence, and S. L. Diamond. 2004. Neutrophil string formation: hydrodynamic thresholding and cellular deformation during cell collisions. *Biophys. J*. 86:4030–4039.

63. Lawrence, M. B., D. F. Bainton, and T. A. Springer. 1994. Neutrophil tethering to and rolling on E-selectin are separable by a requirement for L-selectin. *Immunity*. 1:137–145.